Interference Cancellation and Suppression in Asynchronous Cooperating Base Station Systems

Vincent Kotzsch, Wolfgang Rave and Gerhard Fettweis

Vodafone Chair Mobile Communications Systems, TU-Dresden, Germany
Email: {vincent.kotzsch, rave, fettweis}@ifn.et.tu-dresden.de

***Abstract*—We consider cooperating base station systems where the users are not aligned in time and frequency to the core network as it is actually desired for coherent joint signal processing. As it is widely known, time and frequency offsets can cause inter-symbol as well as inter-carrier interference in OFDM systems which leads to a reduced transmission performance. In this paper we investigate uplink joint detection algorithms which, in addition to multi-user interference cancellation, reduce the asynchronous interference by using iterative interference cancellation as well as mitigating the additional interference by exploiting spatial diversity. The structure of the asynchronous interference in frequency domain can be exploited to derive algorithms with scalable complexity. As will be seen, particularly the interference suppression algorithm provides very good performance results with only a moderate complexity increase.**

I. Introduction

Cooperating base station (BS) systems have gained a lot of attention within research activities of the wireless communication community, since they might increase the spectral efficiency particularly at cell edges (see e.g. [1]). The feasibility of such systems was recently demonstrated in [2]. Investigations of such systems usually rely on the implicit assumption that all transmitter and receiver stations work synchronously. Practical systems, however, do not operate in perfect synchrony and even with efficient synchronization procedures, it will not be possible to find a sampling window that aligns all signals of interest, arriving with different propagation delays, within the guard interval (cyclic prefix, CP) of the OFDM symbol (see e.g. [3]). As a consequence time differences of arrival (TDOA) exceeding (together with the lengths of the channel impulse responses) the guard interval will violate the basic idea of OFDM to decouple subsequent symbols (see e.g. [4]) and turn the desired circular convolution (between transmit signals and channel impulse responses) back to linear convolution. As a result the orthogonality among subcarriers is destroyed causing inter-carrier (ICI) as well as inter-symbol (ISI) interference. Furthermore, carrier frequency offsets between the local oscillators at the BS's and user terminals shift the subcarrier frequencies w.r.t. to their ideal positions by a certain amount leading to additional ICI as well.

In [5] techniques of asynchronous interference mitigation are described but not in an OFDM context and only for flat fading channels. Iterative ICI and ISI cancellation methods for OFDM systems are e.g. part of the investigations in [6] but only for single link transmissions. The goal of this paper is to investigate interference cancellation as well as suppression algorithms that cope with the additional ICI and ISI distortion terms in addition to the multi-user interference. We concentrate on the data transmission in frequency domain and use a system model which includes all effects of asynchronisms in a corresponding effective channel on each subcarrier. This model is used to study the performance of linear data estimators with and without successive interference cancellation in the spatial as well as spectral domain.

The paper is organized as follows: In section II we derive our underlying extended OFDM system model and provide a brief interference power analysis. In section III a subcarrier-wise linear data estimation is discussed and the impact of Rx diversity is investigated. Techniques of iterative asynchronous interference cancellation are discussed in section IV before in section V concluding remarks summarize the main results.

II. Data Transmission Model

Throughout the paper we use a digital baseband OFDM system model with a subcarrier-wise data transmission[1]. Therefore, a set $\mathcal{Q} \subseteq \{1, \ldots, Q\}$ of subcarriers is used for data transmission with $N_{SC} = |\mathcal{Q}|$ subcarriers in total. We assume a system with K single antenna transmitters and M_R receiving BS's, each equipped with N_R receive antennas. Thus, $M = N_R M_R$ observations of K transmit signals are available. All K users are forced to transmit their data on the same time and frequency resource. To focus on the filter problem for estimating the vector of transmitted data $\underline{X}_{o,q} = [X^1_{o,q} \ \cdots \ X^K_{o,q}]^\mathsf{T}$ on subcarrier q in OFDM symbol o using the vector of observations $\underline{Y}_{o,q} = [Y^1_{o,q} \ \cdots \ Y^M_{o,q}]^\mathsf{T}$ the transmission equation can be stated in compact form as:

$$\underline{Y} = \boldsymbol{Z}\underline{X} + \underbrace{\sum_{l \in \mathcal{Q} \setminus q} \boldsymbol{Z}_{o,l}\underline{X}_{o,l} + \sum_{l \in \mathcal{Q}} \boldsymbol{Z}_{o-1,l}\underline{X}_{o-1,l}}_{\underline{U}} + \underline{V} \quad (1)$$

[1]**Notation:** In order to account for the established notation of time and frequency domain used in OFDM the transform domain variables are distinguished by lower as well as uppercase letters, e.g. x for time and X for frequency domain *signal* variables. Matrices, vectors and scalers are stated as boldface, underlined and plain letters, e.g. $\boldsymbol{x}$, $\underline{x}$ and x. Unless it is otherwise stated the vectors are always defined as column vectors. Random variables are denoted by non-italic sans-serif letters and deterministic variables by italic serif letters, e.g. x and x. The operator $\mathrm{E}_{\mathsf{x}}\{.\}$ expresses the expectation value w.r.t. the random variable x.

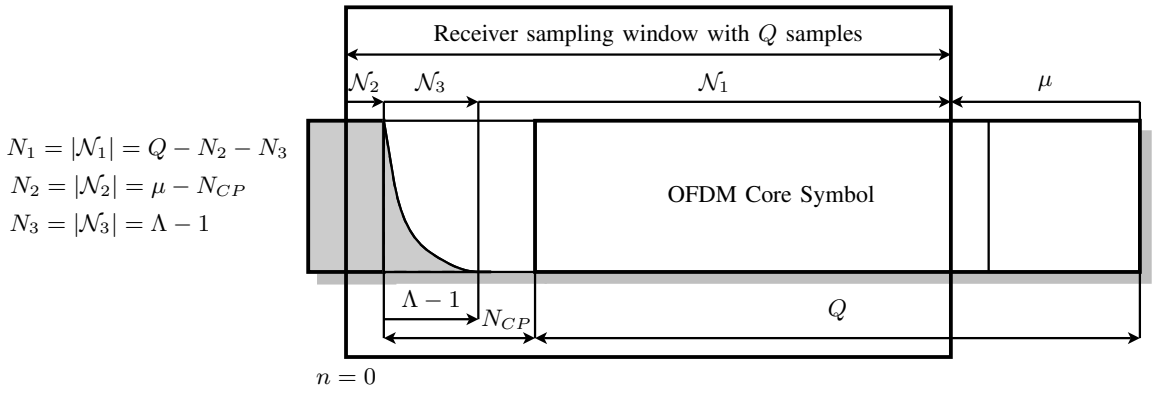

Fig. 1: Possible timing scenario for an unsynchronized user observed at an arbitrary base station with $\mu > N_{CP}$ and $\Lambda > 1$.

For the sake of clarity the indices for the desired OFDM symbol and subcarrier $\{o, q\}$ are omitted throughout the paper. In addition to the spatial coupling of the channel input signals indicated by the effective channel matrix $\boldsymbol{Z} \in \mathbb{C}^{M \times K}$ there is now also a coupling between adjacent subcarriers and OFDM symbols which is referred to as asynchronous interference and is condensed into a vector $\underline{U} \in \mathbb{C}^{M \times 1}$. The additive white Gaussian noise (AWGN) distortion is represented by the vector $\underline{V}$ with $\underline{\mathsf{V}} \propto \mathcal{N}_{\mathbb{C}}\{0, \Phi_{\mathsf{VV}}\}$ and $\Phi_{\mathsf{VV}} = \sigma_V^2 \underline{I}$.

The transmit data symbols X are taken from a discrete symbol alphabet $\mathcal{A} \subset \mathbb{C}$ with $N_M = |\mathcal{A}|$ possible (complex) transmit symbols in total. Throughout this work always a N_M-QAM alphabet is used. If coding is applied a information bit vector $\underline{b} \in \mathbb{F}_2^{N_I \times 1}$ is mapped onto unique codewords $\underline{c} \in \mathbb{F}_2^{N_C \times 1}$ with code rate $R = N_I/N_C$. After interleaving the codeword bits are mapped onto the N_M-QAM constellation points X by using Gray mapping. It should be noted that throughout this work it is always assumed that the interleaved codewords bits are independent uniformly distributed.

A. Asynchronous Interference Model

As mentioned before, the goal of this paper is to analyze techniques for interference cancellation in *frequency* domain. In Eq. (1) a subcarrier-wise coupling model is introduced where $\boldsymbol{Z}_{o,l} = \left[\underline{Z}_{o,l}^1 \cdots \underline{Z}_{o,l}^k \cdots \underline{Z}_{o,l}^K\right]$ denotes the user coupling between the space (index k), frequency (index l) and time (index o). A suitable coupling model with time and frequency asynchronisms is e.g. derived in [7]. In the following a brief sketch of the model derivation is shown in order to get an idea of the dominant ICI and ISI terms. The investigated time and frequency asynchronisms are induced in time domain. Therefore the starting point is the discrete time domain transmission model which can be stated as:

$$y_{o,n}^m = \sum_{k=1}^{K} \sum_{\lambda=1}^{\Lambda^{m,k}} h_\lambda^{m,k} x_{o,n-\mu^{m,k}-\lambda^{m,k}}^k e^{j\Delta\varphi_n^{m,k}} + v_n^m \qquad (2)$$

with n as discrete sample index, k as transmitter and m as receiver index. The transmitted sequence for an OFDM symbol in time domain after the IDFT operation $x_{o,n-\mu^{m,k}}^k$ is delayed by an integer-valued offset $\mu^{m,k} = \left\lfloor \tau_d^{m,k}/T_S \right\rceil$ with $\tau_d^{m,k}$ as the propagation delay between the k-th transmitter and m-th receiver. The variable T_S denotes the sampling period. If for instance a base station synchronization is assumed where the receiver OFDM sampling window is aligned w.r.t. the i-th user the other users are delayed according to their TDOAs $\Delta\tau_d^{m,k} = \tau_d^{m,k} - \tau_d^{m,i}$ and are not synchronized. For those cases the symbol offset μ can also be treated as the corresponding TDOA. The transmit signal is convoluted with the channel impulse response (CIR) $h_\lambda^{m,k}$ which consists of $\Lambda^{m,k} = \left\lfloor \tau_C^{m,k}/T_S \right\rceil$ sampled multi-path components with $\tau_C^{m,k}$ as maximum channel length. The linearly varying phase offset $\Delta\varphi_n^{m,k} = 2\pi\ \Delta\varepsilon^{m,k} n/Q + \varphi_0^{m,k}$ represents the difference of the carrier frequencies between the local oscillators of the transmitter as well as receiver. It is specified as a fraction $\Delta\varepsilon^{m,k}$ of the subcarrier bandwidth.

The received unsynchronized signal samples $y_{o,n}^m$ are transformed into frequency domain by applying the DFT. In Fig. 1 an exemplary timing scenario for an arbitrary user observed at an arbitrary base station is sketched with a timing offset larger than the cyclic prefix length and a frequency selective fading channel. Obviously the signal parts can be split into three regions. While the first region $\mathcal{N}_1$ includes the desired symbol energy, region $\mathcal{N}_2$ only includes non-desired signal portions. In region $\mathcal{N}_3$ due to the channel convolution fractional parts of the desired as well as non-desired OFDM symbols can be observed. As a result, the spectral coupling model can be split into:

$$Y_{o,q}^m = \sum_{k=1}^{K} \left(\sum_{l \in \mathcal{Q}} \underbrace{\left(H_l^{m,k} \Theta_{o,q,l}^{m,k} + \Omega_{o,q,l}^{m,k}\right) e^{\frac{-j2\pi l \mu^{m,k}}{Q}}}_{Z_{o,l}^{m,k}} X_{o,l}^k + \sum_{l \in \mathcal{Q}} \underbrace{\left(H_l^{m,k} \Theta_{o-1,q,l}^{m,k} + \Omega_{o-1,q,l}^{m,k}\right) e^{\frac{-j2\pi l N_2}{Q}}}_{Z_{o-1,l}^{m,k}} X_{o-1,l}^k \right) + V_{o,q}^m \qquad (3)$$

with H_l as the channel transfer function sampled at frequency bin l. The coupling coefficients Θ caused by the windowing in

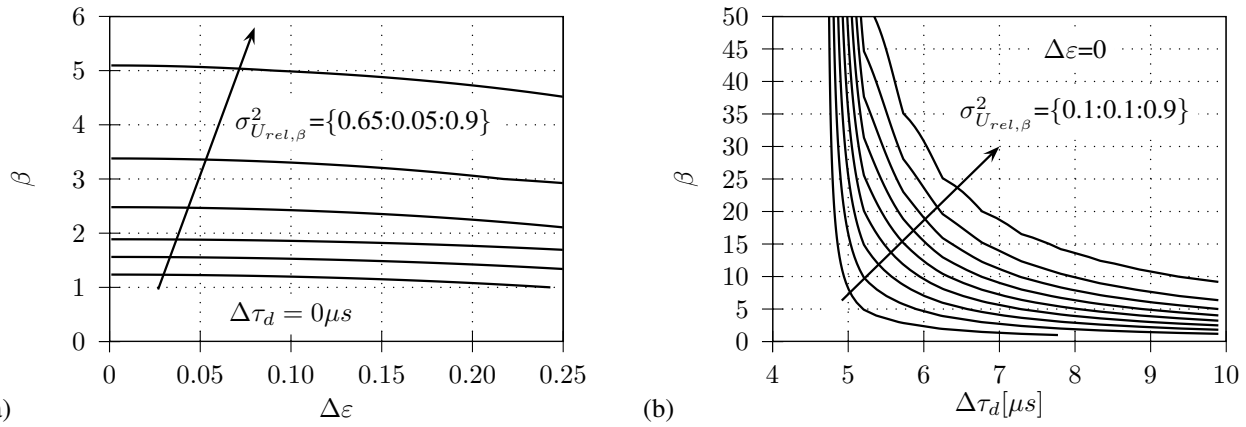

Fig. 2: Contour lines for the relative cumulative ICI power in the desired o-th OFDM symbol for one subcarrier q for an increasing CFO (a) as well as TDOA (b) (OFDM parameters as defined in Tab. I)

region $\mathcal{N}_2$ can be described with the known Dirichlet kernels:

$$\Theta^{m,k}_{o,q,l} = \begin{cases} a^{m,k}/Q & \kappa^{m,k} = 0 \\ \frac{1}{Q} e^{\frac{j\pi}{Q}\phi_o} \frac{\sin\left\{\pi\kappa^{m,k} a^{m,k}/Q\right\}}{\sin\{\pi\kappa^{m,k}/Q\}} & \text{otherwise} \end{cases}$$

$$\Theta^{m,k}_{o-1,q,l} = \begin{cases} b^{m,k}/Q & \kappa^{m,k} = 0 \\ \frac{1}{Q} e^{\frac{j\pi}{Q}\phi_{o-1}} \frac{\sin\left\{\pi\kappa^{m,k} b^{m,k}/Q\right\}}{\sin\{\pi\kappa^{m,k}/Q\}} & \text{otherwise} \end{cases}$$

with $\kappa^{m,k} = l - q + \Delta\varepsilon^{m,k}$ and the corresponding phase terms:

$$\begin{aligned} \phi_o = \; & 2(o(Q+N_{CP})+N_{CP})\Delta\varepsilon^{m,k} \\ & + 2\kappa^{m,k}(b^{m,k}+N_3^{m,k}) + \kappa^{m,k}(a^{m,k}-1) \\ \phi_{o-1} = \; & 2(o(Q+N_{CP})+N_{CP})\Delta\varepsilon^{m,k} + \kappa^{m,k}(b^{m,k}-1) \end{aligned}$$

as well as $a^{m,k} = N_1^{m,k}$ and $b^{m,k} = N_2^{m,k}$.

The other coupling coefficients Ω represent the convolution terms in region $\mathcal{N}_3$ and can be obtained by:

$$\Omega^{m,k}_{o,q,l} = \sum_{n=N_2^{m,k}-1}^{\Lambda+N_2^{m,k}-2} \xi_n^{m,k} \sum_{\lambda=1}^{n-N_2^{m,k}+1} h_\lambda^{m,k} e^{\frac{-j2\pi l\lambda}{Q}}$$

$$\Omega^{m,k}_{o-1,q,l} = \sum_{n=N_2^{m,k}-1}^{\Lambda+N_2^{m,k}-2} \xi_n^{m,k} \sum_{\lambda=n-N_2^{m,k}+1}^{\Lambda-1} h_\lambda^{m,k} e^{\frac{-j2\pi l\lambda}{Q}}$$

with $\xi_n^{m,k} = \exp\left\{j2\pi\kappa^{m,k}n/Q + j\varphi_0^{m,k}\right\}/Q$. For scenarios with fractional ISI ($\mu < N_{CP}$) all variables must be adapted accordingly. It should be noted that in the case of a flat channel ($\Lambda = 1$) the convolution is reduced to a simple multiplication with the channel fading coefficient so that $\Omega^{m,k}_{o,q,l} = \Omega^{m,k}_{o-1,q,l} = 0 \;\forall\; l,q,o$ which simplifies the analysis significantly.

B. Adjacent Subcarriers Interference Power

For the interference cancellation algorithms it is useful to know how much each subcarrier contributes to the total asynchronous interference power. For deriving such an interference power model Eq. (3) needs to be analyzed w.r.t. to the signal power of the desired q-th subcarrier in the o-th OFDM symbol. Unfortunately, due to the convolution terms included into the coupling coefficients $\Omega^{m,k}_{o,q,l}$ and $\Omega^{m,k}_{o-1,q,l}$ this analysis becomes intractable. But one can show that particularly for large Q and small Λ the subcarrier coupling is dominated by the Dirchlet kernels. Thus, for an approximation of the subcarrier coupling powers the convolution terms can simply be ignored which is similar to the flat channel case. The loss of signal power within the o-th OFDM symbol for one subcarrier q can then be obtained by:

$$\sigma^2_{U^{m,k}_{max}} = \frac{a^{m,k}}{Q} - \left|\Theta^{m,k}_{o,q,q}\right|^2 = \frac{a^{m,k}}{Q} - \frac{1}{Q^2}\frac{\sin\left\{\Delta\varepsilon^{m,k}/c^{m,k}\right\}}{\sin\left\{\pi\Delta\varepsilon^{m,k}/Q\right\}}$$

with $c^{m,k} = Q/\pi/a^{m,k}$. The cumulative interference power from the neighboring subcarriers in the o-th OFDM symbol can be stated as:

$$\begin{aligned} \sigma^2_{U^{m,k}_{cum,\beta}} &= \sum_{l=1}^{\beta} \left|\Theta^{m,k}_{o,q+l}\right|^2 + \left|\Theta^{m,k}_{o,q-l}\right|^2 \\ &\approx \sum_{l=1}^{\beta} \frac{1}{2\pi^2}\left(\frac{1-\cos\left\{2\frac{\Delta\varepsilon^{m,k}+l}{c^{m,k}}\right\}}{\left(\Delta\varepsilon^{m,k}/l+1\right)^2 l^2} + \frac{1-\cos\left\{2\frac{\Delta\varepsilon^{m,k}-l}{c^{m,k}}\right\}}{\left(\Delta\varepsilon^{m,k}/l-1\right)^2 l^2}\right) \end{aligned}$$

with $\beta \leq N_{SC}/2 - 1$ as the number or adjacent subcarriers which contribute to maximum interference power. The relative cumulative interference power contribution is then given by $\sigma^2_{U^{m,k}_{rel,\beta}} = \sigma^2_{U^{m,k}_{cum,\beta}}/\sigma^2_{U^{m,k}_{max}}$.

As the previous expressions are not solvable in closed form numerical simulations must be used to evaluate the relative cumulative interference power. This is shown in Fig. 2 for an increasing TDOA as well as CFO. Is should be noted that unless it is otherwise stated always the system parameters

TABLE I: Simulation Parameters

Parameter	Value
System Bandwidth $B_S = 1/T_S$	1.92 MHz
DFT Size Q / CP Length N_{CP}	128 (66.7μs) / 9 (4.7μs)
Used data subcarriers N_{SC}	120
Number of users (K) / BSs (M_R)	2 / 2

defined in Tab. I are used for the numerical simulations throughout this paper. When looking at the simulation results for different CFO values in Fig. 2a one can observe that for reasonable CFOs in the range of $\Delta\varepsilon \approx 0 \ldots 0.05$ the number of subcarriers where the most asynchronous interference power is concentrated remains relatively constant. Only for very large CFOs the interference power contribution slightly changes. For that reason it can be concluded that for the suppression of the ICI caused by the CFO effectively only up to six adjacent subcarriers need to be considered. This picture changes when looking at the simulation results for the timing delays in Fig. 2b. There it can be observed that the number of subcarriers which produce the most asynchronous interference depend on the timing delay. While for low timing delays the interference power is spread over a large bandwidth for an increasing delay the interference power distribution becomes more concentrated onto the 15-20 neighboring subcarriers. The reason for that can be explained with the exponential shape of the underlying Dirichlet kernel. Due to the stretching of the Dirichlet function for the simulated timing delays the adjacent function maxima apart from the main maximum decay quite fast in the region of the neighboring subcarrier frequencies.

III. Asynchronous Interference Suppression

In Eq. (1) a subcarrier based transmission model was introduced which corresponds to the standard processing when considering OFDM systems. One could also use a complete linear matrix vector transmission model with $\underline{Y}' = \boldsymbol{Z}'\underline{X}' + \underline{V}'$ that includes the couplings among all subcarriers, OFDM symbols as well as users completely in $\boldsymbol{Z}'$. But then the transmit signals for each dimension must be stacked into one vector so that $\underline{X}' \in \mathbb{C}^{2N_{SC}K\times 1}$, $\boldsymbol{Z}' \in \mathbb{C}^{N_{SC}M\times 2N_{SC}K}$ and $\underline{Y}' \in \mathbb{C}^{N_{SC}M\times 1}$. As a matrix inversion has a complexity order $\mathcal{O}\left\{N^3\right\}$ one can easily see that although this transmission model would represent the best approach for deriving all types of receive filters the obtained solutions are of infeasible complexity for reasonable parameter sets. Thus, suboptimal filters with less complexity need to be derived which is done in the following.

A. Linear Data Estimation Filters

We can also apply standard results from linear estimation theory to the condensed form of our transmission model in Eq. (1). A linear data estimation filter $\boldsymbol{G}$ aims at suppressing the undesired asynchronous multi-user interference with:

$$\widehat{\underline{\mathsf{X}}} = \boldsymbol{G}\boldsymbol{Z}\underline{\mathsf{X}} + \boldsymbol{G}\underline{\mathsf{U}} + \boldsymbol{G}\underline{\mathsf{V}} \tag{4}$$

The error covariance matrix between the estimated and the transmitted symbols can then be stated as:

$$\begin{aligned}\boldsymbol{\Phi}_{ee} &= \mathrm{E}_{\mathsf{XV}}\left\{\left|\underline{\mathsf{X}} - \widehat{\underline{\mathsf{X}}}\right|^2\right\} \\ &= (\boldsymbol{G}\boldsymbol{Z} - \boldsymbol{I})\left(\boldsymbol{Z}^{\mathrm{H}}\boldsymbol{G}^{\mathrm{H}} - \boldsymbol{I}\right) + \boldsymbol{G}\left(\boldsymbol{\Phi}_{\mathsf{UU}} + \boldsymbol{\Phi}_{\mathsf{VV}}\right)\boldsymbol{G}^{\mathrm{H}}\end{aligned} \tag{5}$$

where it is assumed that $\boldsymbol{\Phi}_{\mathsf{XX}} = \mathrm{E}_{\mathsf{X}}\left\{\underline{\mathsf{X}}\underline{\mathsf{X}}^{\mathrm{H}}\right\} = \boldsymbol{I}$. The asynchronous interference covariance matrix is given by:

$$\boldsymbol{\Phi}_{\mathsf{UU}} = \mathrm{E}_{\mathsf{X}}\left\{\underline{\mathsf{U}}\underline{\mathsf{U}}^{\mathrm{H}}\right\} = \sum_{l\in\mathcal{Q}\setminus q}\boldsymbol{Z}_{o,l}\boldsymbol{Z}_{o,l}^{\mathrm{H}} + \sum_{l\in\mathcal{Q}}\boldsymbol{Z}_{o-1,l}\boldsymbol{Z}_{o-1,l}^{\mathrm{H}} \tag{6}$$

Hence, one can define an effective noise covariance matrix $\boldsymbol{\Phi}_{\widetilde{\mathsf{V}}\widetilde{\mathsf{V}}} = \boldsymbol{\Phi}_{\mathsf{UU}} + \boldsymbol{\Phi}_{\mathsf{VV}}$ which is *not* white anymore.

The optimal linear filter that minimizes the expected mean-square error (MSE) $\boldsymbol{\Phi}_{ee}$ is given by the linear least mean-squares (LLMS) solution (see e.g. [8]):

$$\boldsymbol{G}_{\mathrm{LLMS}} = \left(\boldsymbol{Z}^H\boldsymbol{\Phi}_{\widetilde{\mathsf{V}}\widetilde{\mathsf{V}}}^{-1}\boldsymbol{Z} + \boldsymbol{I}\right)^{-1}\boldsymbol{Z}^H\boldsymbol{\Phi}_{\widetilde{\mathsf{V}}\widetilde{\mathsf{V}}}^{-1} \tag{7}$$

As it is known, the LLMS filter is always biased. For obtaining the unbiased LLMS estimate each filter output must be rescaled to $\widehat{X}_{ub}^k = \widehat{X}^k\left(\underline{Z}^k\boldsymbol{\Phi}_{\mathsf{YY}}^{-1}\left(\underline{Z}^k\right)^{\mathrm{H}}\right)^{-1}$. It should be noted that for frequency selective channels $\boldsymbol{\Phi}_{\mathsf{UU}}$ differs for each subcarrier so that the filter matrix $\boldsymbol{G}_{\mathrm{LLMS}}$ needs to be computed for each subcarrier *separately*. For comparison reasons also the performance of the suboptimal but simple least-squares (LS) filter is tested. The corresponding filter expression is given by:

$$\boldsymbol{G}_{\mathrm{LS}} = \left(\boldsymbol{Z}^H\boldsymbol{Z}\right)^{-1}\boldsymbol{Z}^H \tag{8}$$

which only aims at canceling the spatial interference for the desired transmit symbol but does not take other interference and noise terms into account to minimize the MSE.

In Fig. 3 the impact of the asynchronous interference to the post equalization SINR for the introduced filter types is shown which is defined as:

$$\Gamma^k = \frac{\left(\underline{\widetilde{G}}^k\right)^{\mathrm{H}}\underline{Z}^k\left(\underline{Z}^k\right)^{\mathrm{H}}\underline{G}^k}{\sum_{i=1,i\neq k}^{K}\left(\underline{\widetilde{G}}^k\right)^{\mathrm{H}}\underline{Z}^i\left(\underline{Z}^i\right)^{\mathrm{H}}\underline{G}^k + \left(\underline{\widetilde{G}}^k\right)^{\mathrm{H}}\boldsymbol{\Phi}_{\widetilde{\mathsf{V}}\widetilde{\mathsf{V}}}\underline{G}^k}$$

with $\underline{\widetilde{G}}^k$ as the k-th column vector of the matrix $\widetilde{\boldsymbol{G}} = \boldsymbol{G}^{\mathrm{H}}$.

For the performance evaluation a simple 2x2 symmetric user positioning model is assumed where two users move from the cell border ($\Delta\tau_d = 0$) to their serving base stations which are located at an inter-site distance of 5000m ($\Delta\tau_d = \mathrm{ISD}/c_{light}$). Each base station applies a time and frequency synchronization w.r.t. to the direct user so that at one base station always one aligned and one unaligned user can be observed. Due to the symmetrical user positioning the SINR performance is equal for each user so that the expectation value is jointly taken for the SINR performance of both users within the cooperation cluster. It should be noted that the results always show the *average* performance for all simulated realizations of the CIR. The fading coefficients of the CIR are randomly distributed with $\mathsf{h}_\lambda \propto \mathcal{N}_{\mathbb{C}}\left\{0, \sigma_{h_\lambda}^2\right\}$ and $\sigma_{h_\lambda}^2$ as the corresponding tap power related to the power delay profile. For the sake of simplicity in this paper only uniformly distributed tap powers are used when evaluating frequency selective channels.

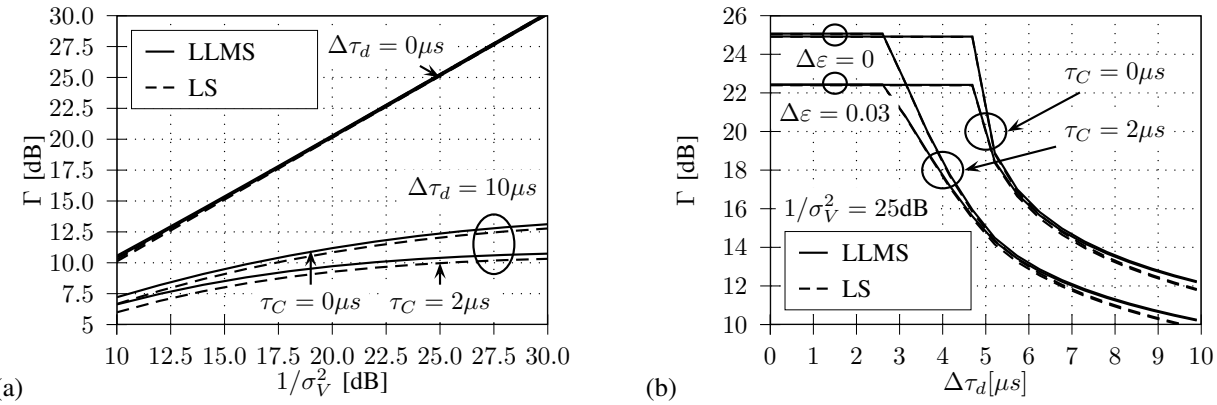

Fig. 3: Average post equalization SINR for an increasing noise power (a) and an increasing TDOA (b) for different values of channel lengths as well as CFOs (OFDM parameters as defined in Tab. I, $N_R = 1$, $\beta = Q/2 - 1$).

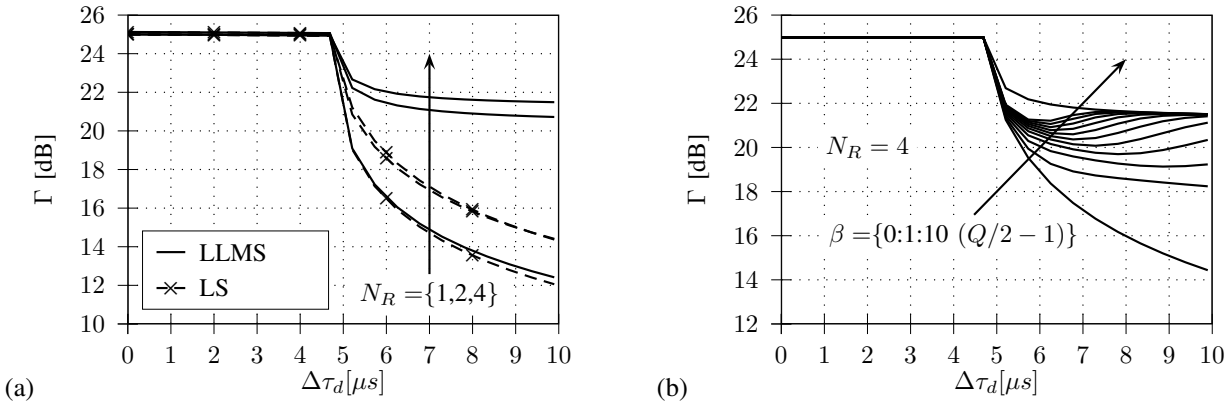

Fig. 4: Impact of the Rx diversity on the average post equalization SINR (a) and impact of the number of most interfering subcarriers included into $\mathbf{\Phi}_{\mathsf{UU}}$ of the LLMS filter (b). (OFDM parameters as defined in Tab. I, $\tau_C = 0\mu s$, $1/\sigma_V^2 = 25$dB).

In Fig. 3a at first the target SNR is varied for two fixed values of TDOAs as well as channel lengths. As reference curve the performance for a zero delay ($\Delta\tau_d = 0\mu$s) is depicted. As expected, one can observe that in this case the post equalization SINR follows exactly the target SNR. Furthermore, as known from estimation theory for low SNR values the LLMS filter reveals a better performance than the LS due to the incorporation of the noise power. For a TDOA value of $\Delta\tau_d = 10\mu$s this gain becomes slightly larger as the effective colored noise covariance leads to noise enhancement. However, one can clearly see the high SNR degradation for both filter types which is ≈15dB for $1/\sigma_V^2 = 30$dB. For an exemplary channel length of $\tau_C = 2\mu$s ($\Lambda = 5$) the SNR degradation also increases further on which leads to additional SNR degradation of ≈2.5dB for $1/\sigma_V^2 = 30$dB.

On the right-hand side of Fig. 3 for a fixed target SNR of 25dB the post equalization SINR for an increasing TDOA is shown for two different channel lengths and CFO values. Again, one can observe that the LLMS filter is always slightly better than the LS implementation but the gain is rather small compared to the actual performance loss. Clearly, as the CFO is not distance dependent it leads to a additional constant SINR degradation for all TDOAs.

B. Interference Suppression with Rx Diversity

As mentioned above, the data estimation filter $\boldsymbol{G}$ primarily aims at canceling synchronous multi-user interference. The number of channel inputs K must always be less or equal than the number of observations at the channel output M. If the number of observations is larger than the number of signals that should be detected the spatial diversity leads to array as well as diversity gain. In most common cellular wireless networks the number of base station antennas is usually larger than one so that one can expect that there are always more observations available than users which transmit on the same resource. As was already shown in [9], the full interference aware LLMS filter can efficiently suppress additional interference terms in the case of Rx diversity. Therefore, in the following the impact of exploiting Rx diversity with the LLMS filter is investigated in numerical simulations. It should be noted that the LLMS filter is not changed in its basic computation.

In Fig. 4a an SINR comparison of the two filter implementations is shown when increasing the number of base station receive antennas N_R. It should be noted that for reasons of comparison for these simulation results the channel gain is scaled according to the Rx diversity degree in order to focus

only on the diversity gain and not on the array gain which would lead to different SINR reference levels for each Rx diversity degree. As one can observe on the left-hand side of the figure particularly the LLMS solution yields always the best results since the *full* asynchronous interference covariance matrix is included into the filter computation. As expected, the LS solution only slightly benefits from the Rx diversity. The LLMS filter does not necessarily need to include all interfering subcarriers into the asynchronous interference covariance matrix $\mathbf{\Phi}_{\mathsf{UU}}$ since particularly for large Q this would result in a high complexity. In Fig. 4b results for the LLMS filter are shown where the number of adjacent subcarriers which are included into $\mathbf{\Phi}_{\mathsf{UU}}$ is successively increased. It should be noted that β denotes the number of adjacent subcarriers from the o-th *and* $(o-1)$-th OFDM symbol of the *two* unaligned links. As one can observe, by including about 10 directly adjacent subcarriers the performance is close to the optimal solution. Furthermore, one can see that the larger the TDOA becomes the smaller the number of neighboring subcarriers is that is needed to achieve the optimal performance. This coincides with the observations derived from Fig. 2b.

IV. Non-Linear Interference Cancellation

In the previous section linear interference suppression filters are investigated which are only a suboptimal approach since they do not exploit additional knowledge about the discrete transmit signal within the observations. This mainly concerns the structure of the codewords and the limited number of constellation points. Therefore in the following, techniques of iterative asynchronous multi-user interference cancellation are discussed for coded transmission where the main idea is to estimate the undesired asynchronous multi-user interference based on already detected transmit symbols which can thereafter be subtracted from the received observations in order to improve the detection performance in subsequent iterations.

A. Iterative Receiver Processing

When using linear equalization filters the estimated transmit symbols are obtained by applying Eq. (4). Already detected symbols $\check{X}^k$ from the initial iteration of the spatial interference cancellation can be used to estimate the asynchronous interference for an iterative interference cancellation. In this context one has to keep in mind that in many cases the symbols of the $(o-1)$-th OFDM symbol are already known. If e.g. one codeword fits into one OFDM symbol it can be assumed that the preceding transmit symbols of each subcarrier are already detected. For such cases one has only to cope with the ICI from the current OFDM symbol. For known symbols of the preceding OFDM symbol $X^k_{o-1,l}$ one can initially subtract the caused interference terms. Hence, the asynchronous interference term U can be estimated iteratively by:

$$\underline{\widehat{U}}^t = \sum_{k=1}^{K} \left(\sum_{l \in \mathcal{Q} \setminus q} \underline{Z}^k_{o,l} \check{X}^{k,t}_{o,l} + \sum_{l \in \mathcal{Q}} \underline{Z}^k_{o-1,l} X^{k,0}_{o-1,l} \right) \quad (9)$$

where the time index $t = 0...t_{max}$ denotes the iteration steps and $\underline{\check{X}}^{k,t}_{o,l} = 0|_{t=0}$. For further iterations the linear LLMS filter introduced in Eq. (7) needs to be recomputed by using the observations $\underline{\widetilde{Y}}^t = \underline{Y} - \underline{\widehat{U}}^{t-1}$. It should be noted that the asynchronous interference covariance which is included into the LLMS filter must also be updated. If $\zeta = X - \check{X}$ denotes the symbol estimation error the input at the linear estimation filter in the t-th iteration can also be stated as:

$$\underline{\widetilde{Y}}^t = \sum_{k=1}^{K} \underline{Z}^k X^{k,t} + \sum_{k=1}^{K} \sum_{l \in \mathcal{Q} \setminus q} \underline{Z}^k_{o,l} \zeta^{k,t}_{o,l} + \underline{V} \quad (10)$$

The LLMS filter matrix must then be calculated by using the augmented noise covariance matrix in the t-th iteration with:

$$\mathbf{\Phi}^t_{\widetilde{\mathsf{V}}\widetilde{\mathsf{V}}} = \mathbf{\Phi}_{\mathsf{VV}} + \mathbf{\Phi}^t_{\mathsf{UU}} = \mathbf{\Phi}_{\mathsf{VV}} + \sum_{l \in \mathcal{Q} \setminus q} \boldsymbol{Z}_{o,l} \mathbf{\Phi}^t_{\zeta\zeta,o,l} \boldsymbol{Z}^{\mathrm{H}}_{o,l} \quad (11)$$

Usually the variance of the data estimation error is not known a-priori but, as will be seen later on, the corresponding terms can be provided by the decoder.

One main performance issue for successful interference cancellation is the correct subtraction of the expected asynchronous multi-user interference. Therefore, usually the decoded information bits are used to estimate the interference parts. As it is known from the literature (see e.g. [10]), iterative receivers which employ soft processing by using only reliability information about the estimated data achieve significantly improved results compared to processing using hard decisions. As summarized in [11] the steps within an iterative receiver with soft processing can be stated as:

- Soft-input soft-output multi-user data estimation
- Soft-input soft-output channel MAP decoding
- Soft interference estimation and subtraction

As only binary digits are transmitted over the communication channel all the information about the codeword bits are included into the so called a-posteriori log-likelihood ratio (APP-LLR)[2]:

$$\mathrm{L}\left\{c^k_i | \underline{Y}\right\} = \ln \left\{ \frac{\Pr\left\{c^k_i = 0 | \underline{Y}\right\}}{\Pr\left\{c^k_i = 1 | \underline{Y}\right\}} \right\} = \mathrm{L}_e\left\{\underline{Y} | c^k_i\right\} + \mathrm{L}_a\left\{c^k_i\right\}$$

which can be split into an extrinsic information part L_e as well as a part L_a which represents a-priori knowledge about the transmitted data. c_i denotes the i-th codeword bit of user k within the received symbol vector $\underline{Y}$.

For linear estimation filters the APP-LLRs must be calculated based on the linear filter outputs for each user separately. One main assumption is to treat the effective noise values as Gaussian distributed which is only a suboptimal but simple approach. The likelihood function which needs to be evaluated

[2]See e.g. [12] for the properties of the L-value algebra.

then becomes:

$$\mathrm{f}_{\widehat{X}^k|\mathsf{c}_i^k}\left\{\widehat{X}^k|c_i^k=\alpha\right\}= \sum_{X^k\in\mathcal{A}:c_i^k=\alpha}\exp\left\{-\frac{\left|\widehat{X}^k-X^k\right|^2}{\widetilde{\sigma}_V^2}-\sum_{o=0,o\neq n}^{\mathrm{ld}\{N_M\}-1}c_o^k\mathrm{L}_a\left\{c_o^k\right\}\right\}$$

with $\alpha\in\{0,1\}$ and L_a as a-priori information available for data estimation. By using the well known Max-Log-APP approximation the APP-LLR can be simplified to:

$$\begin{aligned}\mathrm{L}_e\left\{\widehat{X}^k|c_i^k\right\}\approx &\max_{X^k\in\mathcal{A}:c_i^k=0}\left\{-\frac{\left|\widehat{X}^k-X^k\right|^2}{\widetilde{\sigma}_V^2}-\sum_{o=0,o\neq i}^{\mathrm{ld}\{N_M\}-1}c_o^k\mathrm{L}_a\left\{c_o^k\right\}\right\}\\ &-\max_{X^k\in\mathcal{A}:c_i^k=1}\left\{-\frac{\left|\widehat{X}^k-X^k\right|^2}{\widetilde{\sigma}_V^2}-\sum_{o=0,o\neq i}^{\mathrm{ld}\{N_M\}-1}c_o^k\mathrm{L}_a\left\{c_o^k\right\}\right\}\end{aligned}\tag{12}$$

For the LLMS filter the effective noise variance value can be stated as $\widetilde{\sigma}_V^2=\left(\boldsymbol{Z}_k^{\mathrm{H}}\boldsymbol{\Phi}_{\mathsf{YY}}^{-1}\boldsymbol{Z}_k\right)^{-1}-1$ with $\boldsymbol{\Phi}_{\mathsf{YY}}=\boldsymbol{Z}\boldsymbol{Z}^{\mathrm{H}}+\boldsymbol{\Phi}_{\widetilde{\mathsf{V}}\widetilde{\mathsf{V}}}$.

The extrinsic output information of the data estimator is thereafter passed through the MAP decoder for which typically the BCJR algorithm is used (see e.g. [12]). As mentioned before, the decoder provides hard decisions for the information bits as well as the LLR values for all code bits. The codeword LLR values can be used for soft interference estimation of the data symbols as e.g. described in [13]. The main idea behind this approach is to obtain the most likely transmit symbol based on the decoder output LLR values $\mathrm{L}_a\left\{c_i\right\}$ for each bit of the bit vector that belongs to one complex transmit symbol. The estimated symbol is then given as the expected value for the corresponding bit vector:

$$\check{X}^k=\mathrm{E}\left\{X|\mathrm{L}_a\left\{c_i^k\right\}\right\}=\sum_{o=0}^{N_M-1}\mathcal{A}_o\mathrm{Pr}\left\{X^k=\mathcal{A}_o\right\}\tag{13}$$

with $\mathcal{A}_o$ as o-th element of the symbol alphabet. The variance of the estimation error can be approximated with:

$$\sigma_{\zeta,k}^2=\sum_{o=0}^{N_M-1}\left(\mathcal{A}_o-\check{X}^k\right)^2\mathrm{Pr}\left\{X^k=\mathcal{A}_o\right\}\tag{14}$$

which can be included into the effective noise covariance matrix of the LLMS filter introduced in Eq. (11) with $\boldsymbol{\Phi}_{\zeta\zeta}=\mathrm{diag}\left\{\sigma_{\zeta,0}^2,\ldots,\sigma_{\zeta,K}^2\right\}$. Based on the updated augmented noise covariance matrix $\boldsymbol{\Phi}_{\widetilde{\mathsf{V}}\widetilde{\mathsf{V}}}$ the linear estimation filters must be recalculated for each subcarrier again. After subtracting the estimated asynchronous interference terms from the received signal the entire detection process can be started again.

B. Numerical Simulation Results

For the data transmission a fixed code rate of $R=1/2$ is used with a 16-QAM modulation scheme. As stated in Tab. I in total $N_{SC}=120$ subcarriers are used for data transmission so that in total 480 binary digits can be transmitted within one OFDM symbol. For the sake of simplicity within the simulations the codeword length is also fixed to $N_C=480$ bits so that all OFDM symbols consist always of one codeword.

At the receiver in the first iteration the linear estimation filter according to Eq. (7) with the full asynchronous interference covariance matrix is used to estimate the transmit symbols for each subcarrier. The estimated symbols are thereafter used to compute the LLR values for each codeword bit according to Eq. (12). These codeword LLR values are de-interleaved and provided to the decoder. Within the simulations a 3GPP/LTE compliant coding and interleaving scheme is used as defined in [14] with a recursive systematic convolutional code. Based on the generator polynomial $G=[1,(1+D+D^3)/(1+D^2+D^3)]$ two codewords are concatenated in parallel (with nominal code rate $R=1/3$), punctured to $R=1/2$ and after receive filtering decoded in a turbo decoder using the BJCR algorithm. As mentioned before, the turbo decoder provides the LLR values of all codeword bits. The sign of the LLRs values of the information bits is used as hard decision for the desired bit values. The codeword LLR values after the decoder are interleaved and passed through the soft symbol mapper according to Eq. (13). The soft modulated symbols are used to estimate the asynchronous interference terms according to Eq. (9) which are thereafter be subtracted from the received signal. In further iterations all detection steps, e.g. the recalculation of each linear estimation filter with the updated asynchronous interference covariance matrix stated in Eq. (11), must be carried out for the updated observation vector introduced in Eq. (10).

In Fig. 5 performance results are shown where again the simple 2x2 symmetric user positioning setup is assumed. For all the simulations the average bit error rate is shown. In every simulation run always 500 channel realizations are tested in which always 100 codewords for different noise and input bit realizations are transmitted. In Fig. 5a simulation results for a channel length of $\tau_C=2\mu$s ($\Lambda=5$) are shown. The reference curves are indicated by dashed lines as well as the performance curves for the extended iterative receiver by solid lines. As reference for the decoder performance the AWGN curve is included. Furthermore, the best achievable performance is depicted for $\Delta\tau_d=0\mu$s which represents a scenario where only the spatial multi-user interference must be canceled. Contrary to that, the worst case performance is shown for the case of a fixed TDOA of $\Delta\tau_d=10\mu$s where no iterative detection is applied. For sake of clarity only one TDOA value is tested here which represents the scenario which is also shown in Fig. 3 at the bottom right corner. For investigating the performance of the proposed extended iterative receiver at first two iterations of the entire detection are carried out which is indicated by $t=1$ as well as $t=2$. For these simulations *all* N_{SC} adjacent subcarriers are used for the asynchronous interference estimation. As one can observe, the performance of the iterative interference cancellation is quite close to the best achievable performance for a zero TDOA. By applying more than one receiver iteration one can improve the

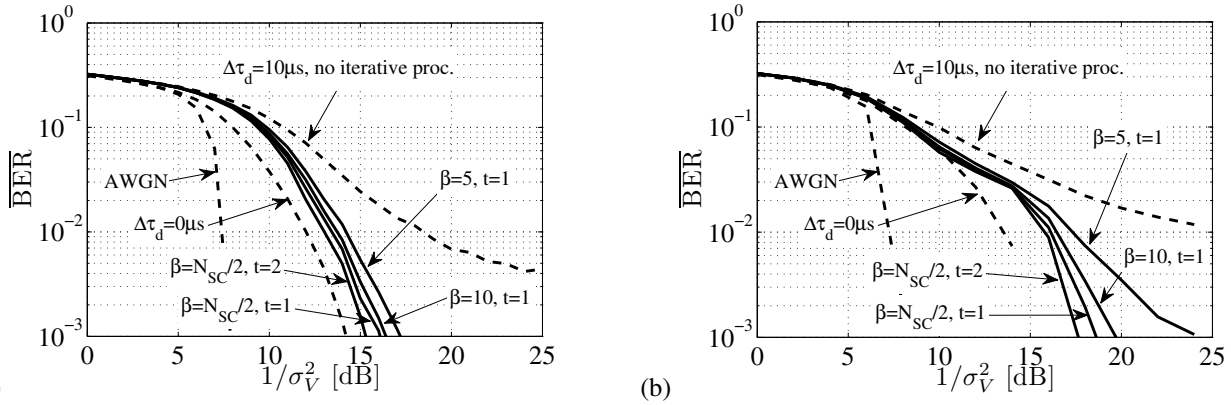

Fig. 5: Average bit error rate performance for $\tau_C = 2\mu$s (a) as well as $\tau_C = 1\mu$s (b) for different interference cancellation strategies (OFDM parameters as defined in Tab. I, $N_R = 1$).

reliability of the estimated data which decreases the bit error rate further on. In order to show how the receiver complexity can be decreased also the number of subcarriers β which are included into the asynchronous interference estimation process is varied. As one can see, as already observed in Fig. 2b as well as in Fig. 4b by including the 10 adjacent subcarrier leads almost to the optimal performance for this simulation case.

In Fig. 5b the same simulation scenarios are tested for a channel length of $\tau_C = 1\mu$s ($\Lambda = 3$). As it is known from the literature, the BER performance depends on the diversity degree. The loss of frequency diversity can be observed in the reduced system performance which leads to a reduced reliability of the estimated user symbols and an increasing error propagation within the iteration steps. But as one can see again, by increasing the number of receiver iterations moderate performance improvements are possible.

V. Conclusion

In this paper we presented an analysis about interference suppression and cancellation for cooperating base station systems where the received signals at the base stations are not coherently superimposed due to the unavoidable TDOAs. A frequency domain transmission model was introduced which includes the dominant distortions caused by time and frequency asynchronisms. Thereafter, this model was used for an extended analysis of linear data estimation algorithms. As shown, by exploiting the Rx diversity the asynchronous interference can be efficiently suppressed. Furthermore, we have shown that also with an extended iterative receiver with soft processing one can alleviate the effect of the asynchronisms significantly. The investigations done in this paper also included an analysis of the dominant subcarrier couplings. It was shown that the most asynchronous interference is generated by the directly adjacent subcarriers. This result can be exploited for designing receivers with scalable complexity. Particularly in scenarios with large inter-site distances the evaluated techniques can be applied in order to increase the system spectral efficiency by avoiding large cyclic prefix lengths. In further work the proposed algorithms need to be evaluated in more practical setups where e.g. also the parameter estimation errors are included into the analysis.

Acknowledgement

The research leading to these results has received funding from the European Commission's seventh framework programme FP7-ICT-2009 under grant agreement no 247223 also referred to as ARTIST4G.

References

[1] D. Gesbert, S. Hanly, H. Huang, S. Shamai Shitz, O. Simeone, and W. Yu, "Multi-Cell MIMO Cooperative Networks: A New Look at Interference," *IEEE J. Sel. Areas Commun.*, vol. 28, no. 9, pp. 1380 –1408, Dec. 2010.

[2] R. Irmer, H. Droste, P. Marsch, M. Grieger, G. Fettweis, S. Brueck, H.-P. Mayer, L. Thiele, and V. Jungnickel, "Coordinated Multipoint: Concepts, Performance, and Field Trial Results," *IEEE Commun. Mag.*, vol. 49, no. 2, pp. 102 –111, Feb. 2011.

[3] M. Morelli, C.-C. J. Kuo, and M.-O. Pun, "Synchronization Techniques for Orthogonal Frequency Division Multiple Access (OFDMA): A Tutorial Review," *Proc. IEEE*, vol. 95, no. 7, Jul. 2007.

[4] Z. Wang and G. B. Giannakis, "Wireless Multicarrier Communications," *IEEE Signal Process. Mag.*, vol. 17, no. 3, May 2000.

[5] H. Zhang, N. B. Mehta, A. F. Molisch, J. Zhang, and H. Dai, "Asynchronous Interference Mitigation in Cooperative Base Station Systems," *IEEE Trans. Wireless Commun.*, vol. 7, no. 1, Jan. 2008.

[6] S. Suyama, H. Suzuki, and K. Fukawa, "An OFDM Receiver Employing Turbo Equalization for Multipath Environments with Delay Spread Greater than the Guard Interval," in *Proc. IEEE Vehicular Technology Conf. (VTC)*, Apr. 2003.

[7] V. Kotzsch and G. Fettweis, "Interference Analysis in Time and Frequency Asynchronous Network MIMO OFDM Systems," in *Proc. IEEE Wireless Commun. and Networking Conf. (WCNC)*, Apr. 2010.

[8] A. H. Sayed, *Adaptive Filters*. J. Wiley & Sons, 2008.

[9] J. Winters, "Optimum Combining in Digital Mobile Radio with Cochannel Interference," *IEEE Trans. Veh. Technol.*, vol. 33, no. 3, Aug. 1984.

[10] H. Lee, B. Lee, and I. Lee, "Iterative Detection and Decoding with an Improved V-BLAST for MIMO-OFDM Systems," *IEEE J. Sel. Areas Commun.*, vol. 24, no. 3, pp. 504 –513, Mar. 2006.

[11] S. Khattak, W. Rave, and G. Fettweis, "Distributed Iterative Multiuser Detection through Base Station Cooperation," *EURASIP Journal on Wireless Commun. and Networking*, 2008.

[12] J. Hagenauer, E. Offer, and L. Papke, "Iterative Decoding of Binary Block and Convolutional Codes," *IEEE Trans. Inf. Theory*, vol. 42, no. 2, pp. 429 –445, Mar. 1996.

[13] W.-J. Choi, K.-W. Cheong, and J. Cioffi, "Iterative Soft Interference Cancellation for Multiple Antenna Systems," in *Proc. IEEE Wireless Commun. and Networking Conf. (WCNC)*, 2000.

[14] 3GPP, *Multiplexing and Channel Coding*, Dec. 2011, tS 36.212 v10.4.0.